

# Study of Transport Regimes in Ion Temperature Gradient Driven Turbulence

TAKEDA Kazuo, BENKADDA Sadruddin<sup>1</sup>,  
HAMAGUCHI Satoshi and WAKATANI Masahiro\*

Kyoto University, Uji, 611-0011, Japan

<sup>1</sup>CNRS URA 773, Université de Provence, France

(Received: 9 December 2003 / Accepted: 23 February 2004)

## Abstract

With a low-degree-of-freedom model composed of 18 ordinary differential equations (ODEs), it is shown that intermittent oscillations are generated by nonlinear interactions between toroidal ion temperature gradient (ITG) driven modes and self-generated sheared flows. The intermittent oscillations are also observed when higher harmonics are included and the number of ODEs is increased up to 56. However, in the cases considered here, if more higher harmonics are included, the saturation level of the kinetic energy becomes lower and the period of intermittency becomes shorter for the same value of the ion pressure gradient.

## Keywords:

ITG-driven turbulence, low-dimensional model, transition, intermittency, avalanche, sheared flow, Nusselt number

## 1. Introduction

The anomalous transport governed by microscopic turbulence is one of the most important issues in the research of magnetically confined plasmas [1]. Ion temperature gradient (ITG) driven turbulence [2-5] is responsible for the anomalous ion thermal transport in the core region of tokamaks as observed in fluid simulations [2,6], gyrofluid simulations [7,8], and gyrokinetic simulations [9].

In order to understand the physics of nonlinear interactions between anomalous transport and sheared plasma flow, we find it useful to analyze low-degree-of-freedom models that describe essential dynamics governed by partial differential equations.

It was shown that dynamics of resistive interchange turbulence is well described by extended Lorenz systems, i.e., coupled ordinary differential equations (ODEs) for low order modes. Takayama *et al.* [10] studied 5,6 and 7 ODE models for resistive interchange turbulence and showed that an ELM-like behaviour is obtained with the generation of sheared flows and suppression of the turbulence.

The ITG mode has intrinsically twice the number of degrees of freedom compared with the resistive interchange turbulence since it contains wave phenomena. Hu and Horton [11] gave an 11 ODE model for toroidal ITG turbulence and discussed transport barrier dynamics with oscillations in kinetic energy such as barrier localized modes (BLM).

This article is organized as follows. In Sec. 2, model

equations describing the toroidal ITG mode are given and its linear stability is analyzed. We also introduce our low-degree-of-freedom models in Sec. 2. In Sec. 3, our numerical simulation results are presented.

## 2. Models

The toroidal ITG-driven turbulence in a slab is described by the following vorticity and ion pressure equations given by Horton, Choi and Tang [3]:

$$\frac{\partial}{\partial t} (\nabla_{\perp}^2 \phi - \phi) + [\phi, \nabla_{\perp}^2 \phi] = (1 - g + K_i \nabla_{\perp}^2) \frac{\partial \phi}{\partial y} - g \frac{\partial p}{\partial y} + \mu \nabla_{\perp}^2 \nabla_{\perp}^2 \phi, \quad (1)$$

$$\frac{\partial p}{\partial t} + [\phi, p] = -K_i \frac{\partial \phi}{\partial y} + \kappa \nabla_{\perp}^2 p, \quad (2)$$

where

$$[a, b] \equiv \frac{\partial a}{\partial x} \frac{\partial b}{\partial y} - \frac{\partial a}{\partial y} \frac{\partial b}{\partial x} \quad (3)$$

are the Poisson brackets. Here  $g = 2L_{\perp}/R$  is the effective gravity due to curvature of magnetic field,  $K_i = T_i/T_e(\eta_i + 1)$  is the equilibrium ion pressure gradient with  $\eta_i = d \ln T_i / d \ln n$ ,  $\mu$  is the viscosity and  $\kappa$  is the thermal conductivity. Here  $x$  and  $y$  correspond to the radial and poloidal directions, respectively.

The standard drift wave units  $x \equiv x/\rho_s$ ,  $y \equiv y/\rho_s$ ,  $t \equiv (L_n/c_s)t$ ,  $p \equiv L_n T_{i0}/(\rho_s P_{i0} T_{e0})p$ ,  $\phi \equiv e L_n/(B_0 T_{e0} \rho_s)\phi$ ,  $\mu \equiv e L_n/(B_0 T_{e0} \rho_s)\mu$ , and  $\kappa \equiv e L_n/(B_0 T_{e0} \rho_s)\kappa$  are used for normalization, where  $c_s$  is the ion sound velocity,  $\rho_s = c_s/\Omega_i$ , and  $\Omega_i$  is the ion cyclotron frequency.

By linearizing Eqs. (1) and (2), the following dispersion relation of the toroidal ITG mode is obtained,

$$[-i(1+k_\perp^2)\omega + ik_y(1-g-K_i k_\perp^2) + \mu k_\perp^2] \times (-i\omega + \kappa k_\perp^2) - g K_i k_y^2 = 0. \quad (4)$$

The dispersion relation (4) gives the linear growth rate as

$$\omega = \frac{1}{2(1+k_\perp^2)} \{k_y(1-g-K_i k_\perp^2) - i[\kappa k_\perp^2(1+k_\perp^2) + \mu k_\perp^4] \pm \sqrt{D_k}\}, \quad (5)$$

where

$$D_k = \{k_y(1-g-K_i k_\perp^2) + i[\kappa k_\perp^2(1+k_\perp^2) - \mu k_\perp^4]\}^2 - 4(1+k_\perp^2)g K_i k_y^2. \quad (6)$$

From Eq. (5), the most unstable mode is estimated as

$$k_x^2 \ll k_y^2 \sim k_\perp^2 = \frac{1-g}{K_i}. \quad (7)$$

Therefore, as the fundamental mode of our numerical simulations, we have selected a mode close to the most unstable mode satisfying

$$k_x = k_y/2 \quad (8)$$

with  $k_x = [(1-g)/5K_i]^{1/2}$  and  $k_y = [4(1-g)/5K_i]^{1/2}$ .

In order to construct low-degree-of-freedom models, variables  $\phi(t, x, y)$  and  $p(t, x, y)$  are expanded as follows,

$$\phi(t, x, y) = \sum_{m_x=1}^{N_x} \sum_{m_y=0}^{N_y} [\hat{\phi}_{m_x, m_y}^c(t) \sin(m_x k_x x) \cos(m_y k_y y) + \hat{\phi}_{m_x, m_y}^s(t) \sin(m_x k_x x) \sin(m_y k_y y)], \quad (9)$$

$$p(t, x, y) = \sum_{m_x=1}^{N_x} \sum_{m_y=0}^{N_y} [\hat{p}_{m_x, m_y}^c(t) \sin(m_x k_x x) \cos(m_y k_y y) + \hat{p}_{m_x, m_y}^s(t) \sin(m_x k_x x) \sin(m_y k_y y)], \quad (10)$$

where  $N_x$  ( $N_y$ ) is the maximum mode number in the  $x$  ( $y$ ) direction. By substituting Eqs. (9) and (10) into Eqs. (1) and (2), we obtain coupled ordinary differential equations (ODEs) for the harmonics. The 11 ODE model given by Hu and Horton [9], which corresponds to  $N_x = 2$  and  $N_y = 1$ , generates an L-H like transition and oscillatory behaviour. However the obtained sheared flow is not strong enough to suppress the ITG turbulence and therefore the transition seems to be weak. So we have increased the degrees of freedom from 11 to 18 ( $N_x = 3$  and  $N_y = 1$ ) [12] and more in order to analyze the anomalous transport and sheared flows generated by nonlinear ITG modes with higher accuracy. In the small  $K_i$  region of  $K_i \leq 3$ , a bifurcation process similar to that

observed in the 11 ODE model also appears in the 18 ODE model. The noteworthy difference between the 11 and 18 ODEs is that, only in the case of 18 (or larger) ODEs, intermittent bursts (so called avalanches) are observed in the time evolution of the kinetic energy and the Nusselt number when  $K_i$  is large. This results from the competition of the three factors, i.e., ITG turbulence that generates sheared flows, the sheared flows that suppress the ITG turbulence, and viscosity that suppresses the sheared flows.

### 3. Numerical results

The kinetic energy due to velocity fluctuations can be calculated from the vorticity equation (1) as

$$K = \int \phi^2 + (\nabla_\perp \phi)^2 dV/V = \langle \phi^2 + (\nabla_\perp \phi)^2 \rangle_V. \quad (11)$$

So the kinetic energy can be calculated separately for shear flow components ( $m_y = 0$  mode) and other harmonic modes as follows

$$K_0 = \sum_{m_x=1}^{N_x} \frac{1}{4} (1 + m_x^2 k_x^2) (\phi_{m_x}^0)^2, \quad (12)$$

$$K_{m_x, m_y} = \frac{1}{8} (1 + m_x^2 k_x^2 + m_y^2 k_y^2) [(\phi_{m_x, m_y}^c)^2 + (\phi_{m_x, m_y}^s)^2]. \quad (13)$$

To characterize the anomalous thermal transport, we also calculated the Nusselt number, which is the ratio of the total heat transport including convective or anomalous transport to the conductive heat transport defined as

$$N_u = 1 + \int p v_x dV / \left( \kappa \frac{dP_0}{dx} \right) = 1 + \frac{\langle p v_x \rangle_V}{\kappa K_i}. \quad (14)$$

Figures 1 and 2 show simulation results for  $K_i = 8$  from the 18 ODE model, which corresponds to  $N_x = 3$  and  $N_y = 1$ . Time evolution of the kinetic energy is shown in Fig. 1.

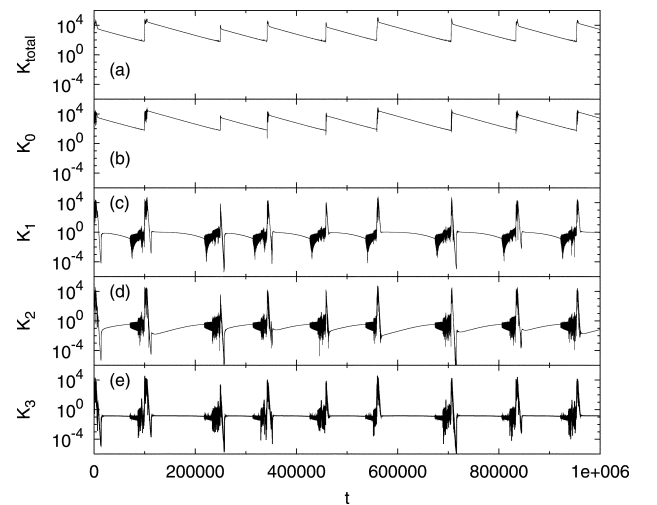


Fig. 1 Time evolution of (a) total kinetic energy and kinetic energy of (b) the sheared flow  $K_0$ , (c) the 1st harmonic  $K_{1,1}$ , (d) the 2nd harmonic  $K_{2,1}$ , and (e) the 3rd harmonic  $K_{3,1}$  in the case of  $N_x = 3$  and  $N_y = 1$  for  $K_i = 8$ .

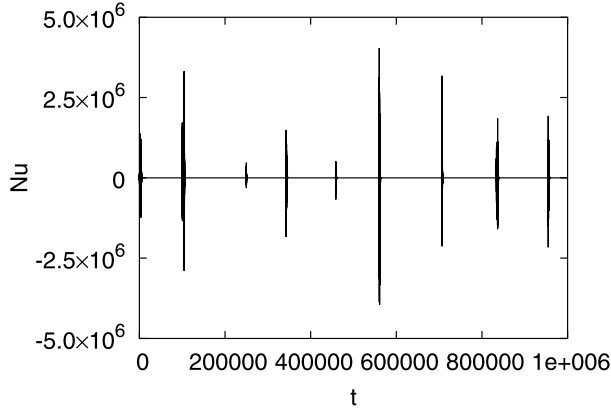


Fig. 2 Time evolution of the Nusselt number in the case of  $N_x = 3$  and  $N_y = 1$  for  $K_i = 8$ .

Intermittent bursts, so called avalanches, are caused by nonlinear interactions between the ITG modes and the sheared flows. As the ITG modes grow, the sheared flows are generated through the Reynolds stress. Sufficiently strong sheared flows can suppress the ITG modes quickly. After the ITG modes are suppressed, with the lack of a flow source, the sheared flows gradually decay due to viscosity. Time evolution of the Nusselt number  $N_u$  is presented in Fig. 2, where one sees that the Nusselt number bursts at the time when the ITG modes grow rapidly.

For comparison, we have also studied the case of  $N_x = 4$  and  $N_y = 3$ . Simulation results for  $N_x = 4$  and  $N_y = 3$  (56 coupled ODEs) are shown in Figs. 3 and 4 for  $K_i = 8$ , i.e., the same value as that of Figs. 1 and 2. Intermittent bursts of the kinetic energy and the Nusselt number fluctuations are also observed. However the saturation level of the kinetic energy is lower and the period of bursts is shorter than those in the case of  $N_x = 3$  and  $N_y = 1$ .

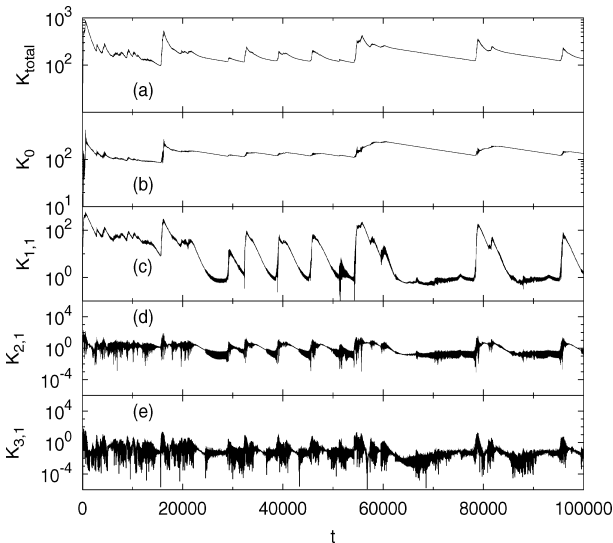


Fig. 3 Time evolution of (a) total kinetic energy and kinetic energy of (b) the sheared flow  $K_0$ , (c)  $K_{1,1}$ , (d)  $K_{2,1}$ , and (e)  $K_{3,1}$  in the case of  $N_x = 4$  and  $N_y = 3$  for  $K_i = 8$ .

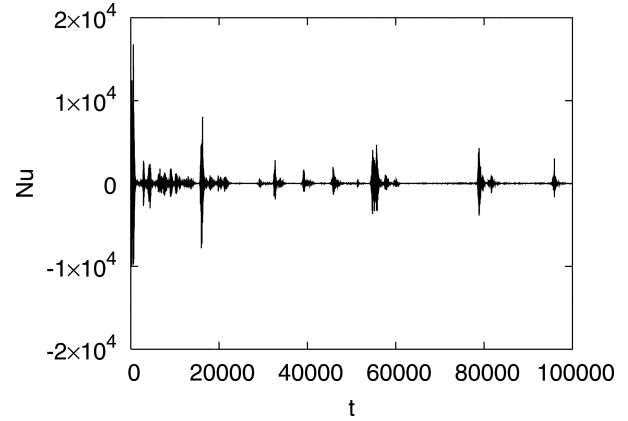


Fig. 4 Time evolution of the Nusselt number in the case of  $N_x = 4$  and  $N_y = 3$  for  $K_i = 8$ .

In summary, it is verified that the essential nonlinear behaviour of the system can be at least qualitatively accounted for by nonlinear interactions of several low order harmonics. We also find that such intermittent bursts also occur in our model of the 24 ODEs ( $N_x = 4$  and  $N_y = 1$ ), the 30 ODEs ( $N_x = 3$  and  $N_y = 2$ ), and the 40 ODEs ( $N_x = 4$  and  $N_y = 2$ ) although their saturation levels and the periods of bursts are different. Among these cases, the mode saturation levels and burst periods decrease as the number of higher modes included in the ODE model increases. These quantities may converge to certain values when we increase the degrees of freedom. We believe these models, which contain the most unstable mode and several low-order harmonic modes, are likely to capture the essential dynamical effects of the original physical system.

\* deceased

## References

- [1] ITER Physics Basis, Nucl. Fusion **39**, 2137 (1999).
- [2] S. Hamaguchi and W. Horton, Phys. Fluids B **2**, 1834 (1990).
- [3] W. Horton, D.-I. Choi and W. Tang, Phys. Fluids **24**, 1077 (1981).
- [4] W. Horton, R.D. Estes and D. Biskamp, Plasma Phys. **22**, 663 (1980).
- [5] A. Jarmen, P. Andersson and J. Weiland, Nucl. Fusion **27**, 941 (1987).
- [6] H. Mordman and J. Weiland, Nucl. Fusion **29**, 251 (1989).
- [7] G.W. Hammett and F.W. Perkins, Phys. Rev. Lett. **64**, 3019 (1990).
- [8] M.A. Beer and G.W. Hammett, Phys. Plasmas **3**, 4046 (1996).
- [9] A.M. Dimit *et al.*, Phys. Plasmas **7**, 969 (2000).
- [10] A. Takayama, T. Unemura and M. Wakatani, Plasma Phys. Control. Fusion **40**, 775 (1998).
- [11] G. Hu and W. Horton, Phys. Plasmas **3**, 3262 (1997).
- [12] K. Takeda, S. Hamaguchi and M. Wakatani, Plasma Phys. Control. Fusion **44**, A487 (2002).